Surfaces and Interfaces 28 (2022) 101686

Contents lists available at ScienceDirect

Surfaces and Interfaces

journal homepage: www.sciencedirect.com/journal/surfaces-and-interfaces

Atomic layer deposition coated polymer films with enhanced high-temperature dielectric strength suitable for film capacitors

Xudong Wu [a,b], Yichen Liu [a], Xiaotian Lin [a], Enling Huang [a], Guanghui Song [a], Daniel Q. Tan [a,c,*]

[a] Department of Materials Science and Engineering, Guangdong Technion Israel Institute of Technology, 241 Daxue Road, Shantou 515063, PR China
[b] Department of Materials Science and Engineering, Technion - Israel Institute of Technology, Haifa 3200003, Israel
[c] Guangdong Provincial Key Laboratory of Materials and Technology for Energy Conversion, 241 Daxue Road, Shantou 515063, PR China

ARTICLE INFO

Keywords:
Polymer films
High temperature
Breakdown strength
Atomic layer deposition
Energy density

ABSTRACT

Although polymer film capacitors are widely used in power electronic systems, their high-temperature performance deterioration severely limits their further application. This work shows conclusively that ultrathin alumina coating by atomic layer deposition (ALD) can significantly improve the thermal stability and capacitance stability of polypropylene (PP) films at temperatures above 140 ℃. We demonstrate for the first time the ALD coating enhancement on breakdown strength (>600 V/μm) and elastic modulus of both crystalline PP and amorphous polyetherimide (PEI) at higher temperatures. The discharged energy density of ALD alumina-coated PP and PEI films reached 4.1 J/cm^3 at 140 ℃, 2.6 J/cm^3 at 150 ℃, respectively, which is much higher than uncoated films. The finite element simulation also manifests the consistency in dielectric strength enhancement that may be attributed to the increased elastic modulus due to the alumina coating. This new perspective provides an effective pathway to obtain ultrathin surface coating for dielectric polymer films with enhanced dielectric strength, elastic modulus, and thermal stability promising higher temperature application.

1. Introduction

Polymer film capacitors are characteristic of excellent operational life performance due to the weak or non-polarity, high electrical resistance, wide frequency response, high breakdown strength, low dielectric loss, and graceful failure merit. These advantages deliver film capacitors in applications requiring high voltage, high current, and high-temperature environments such as aviation/avionics, automobile/transportation, power transmission/national grid, oil and gas exploration, and advanced propulsion systems [1–4]. The increased operation temperature and heating problem caused by the miniaturization of electronic components and the increase of power consumption forced the development of high-temperature-resistant polymeric materials and their capacitor technologies [5,6]. For instance, in hybrid electric vehicles, the temperature under the hood may exceed 140 ℃. Their inverters, as important modules consisting of film capacitors, convert the direct current (DC) power of the battery to the alternating current (AC) power to drive the traction motor. Mainstream capacitor manufacturers currently use biaxial oriented polypropylene (BOPP) as the dielectric in the power inverters, which needs about 40% of the volume and 23% of the weight for capacitors. Yet, the bulky BOPP capacitor limited to 105 ℃ cannot meet the ambient temperature requirement of a hybrid vehicle. The design engineers still prefer to use BOPP capacitors for superior dielectric performance in the module and system design by introducing a secondary cooling system for the power inverter [7–9]. The assistant auxiliary cooling loop brings additional weight, volume, and complexity to the electrical system design, which cause higher manufacturing cost and reduced vehicle performance.

In recent years, many research has explored high-temperature resistant polymers or composites [10–12]. However, the road from the laboratory to the industry is a long journey, which involves a trade-off of dielectric properties, scale-up challenges, cost-effectiveness, and comprehensive technical integrity. Consequently, BOPP capacitors remain the footstone of the film capacitor technology and are attractive to continued improvement and innovation. One method is the chemical modification of PP by melt grafting, high-energy carbon ions, decomposition of unsaturated peroxides [13–15]. Yet, the property improvement at higher temperatures has not been satisfactory. Zhou et al. [16] fabricated PP-mah-MgO/PP nanocomposites and showed a stable dielectric constant, decreased dielectric loss, and improved breakdown

* Corresponding author at: Department of Materials Science and Engineering, Guangdong Technion Israel Institute of Technology, 241 Daxue Road, Shantou 515063, PR China.
E-mail address: daniel.tan@gtiit.edu.cn (D.Q. Tan).

https://doi.org/10.1016/j.surfin.2021.101686
Received 22 October 2021; Received in revised form 10 December 2021; Accepted 13 December 2021
Available online 16 December 2021

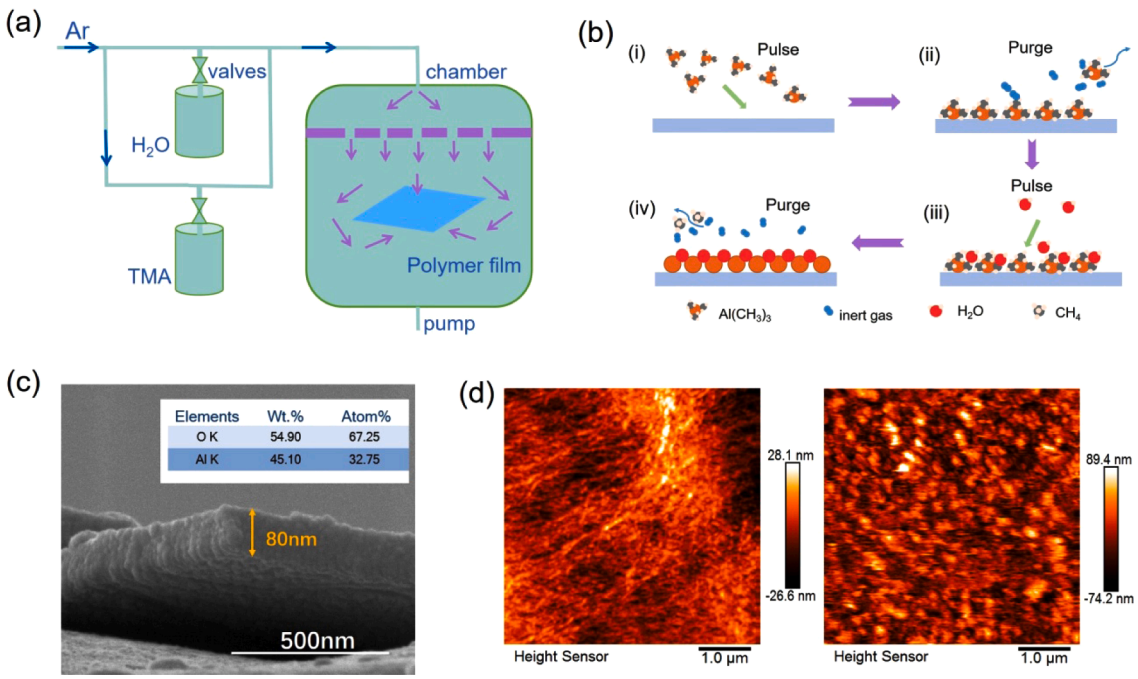

Fig. 1. (a) Schematic diagram of ALD deposited Al_2O_3. (b) Mechanistic diagram of ALD deposition process. (c) SEM image of Al_2O_3 layer and elements analysis. (d) AFM images of PP film (left) and PP coated Al_2O_3 film (right) surface.

strength. The prepared PP nanocomposites display a discharged energy density of 1.66 J/cm^3 at 400 MV/m at 120 ℃. Although some PP films may be electrically tested at temperatures above 120 ℃, the films exhibit a great change in dimensions and are not suitable for capacitor fabrication and operation. The feasibility of extending PP films to higher temperatures still requires more investigation and innovation in terms of processing simplicity, thermal stability, and dielectric strength of the films at elevated temperatures.

The Atomic layer deposition (ALD) method is an excellent surface coating technique that deposits inorganic compound atoms layer by layer. It not only helps to reduce defect influence of the roughness and thus exhibit the intrinsic properties of the polymer films but also reduces the dimensional film changes occurring at elevated temperatures [17, 18]. This method takes advantage of commercially manufactured PP films of various characteristics. It does not involve more complicated scale-up processes of nanoparticle-filled polymers or lengthy technical challenges in new monomer development. The plasma-enhanced chemical vapor deposition (PECVD) method also shows a positive effect on improving the dielectric strength of polyetherimide (PEI) at above 100 ℃ using a BN coating of high thermal conductivity [19]. In light of the previously reported feasibility of property improvement at room temperature using film surface coating, it is desirable to further apply the ALD method for more dielectric strength improvement at higher temperatures and the physical mechanism of the enhancement in the strategically critical dielectric polymers of polypropylene and PEI.

This work applies the oxide coating using ALD to enhance the thermal stability, the dielectric breakdown strength, and the energy storage capability at elevated temperatures. The breakdown strength of the alumina-coated crystalline PP film increases to 600 V/μm and the discharged energy density improves to 4.1 J/cm^3 at 140 ℃. The discharge energy density of the alumina-coated amorphous PEI also increases to 2.6 J/cm^3 at 600 V/μm when tested at 150 ℃. The work also carried out a computer simulation to explain the observed phenomena. This surface modification strategy may provide a feasible scheme to raise the operating temperatures of various dielectric polymer films and to design high temperature-resistant film capacitors.

2. Experimental

2.1. Films and chemicals

The 5.8 μm PP and 5 μm PEI films were provided by Steinerfilm USA and Bollore USA, respectively. Trimethyl aluminum (TMA) and H_2O were provided as Al and O precursors during the ALD of Al_2O_3. Precursor TMA was supplied by Nanjing Ai Mou Yuan Scientific Equipment Co., Ltd with 99.99% purity. H_2O was from a pure water system.

2.2. ALD experimental

ALD alumina coating on the PP and PEI films was done using a benchtop GEMSTAR TX ALD system (Arradiance Inc., Sudbury, MA USA) with automated control to the alternate precursor pulsing and inert gas purging steps. Argon gas was used as carrier and purging gases and flowed into the ALD chamber with a 10sccm flow rate. The ALD chamber was pumped down to a 254 mTorr vacuum and heated up to 90–100 ℃ before ALD starts. Al_2O_3 nanolayer on polymer films was deposited at 70 ℃, with each cycle dosed TMA pulse/argon flushing/H_2O pulse/argon flushing for the period of 21 ms, 6 s, 21 ms, and 6 s, respectively.

2.3. Characterization

The surface morphology of the polymer films was investigated using ZEISS Sigma-500 (Germany) Field Emission Scanning Electron Microscopy (FESEM) and Bruker Dimension (Germany) Atomic Force Microscope (AFM). Transmission electron microscopy (TEM) images were captured by an FEI Talos F200X G2 (USA) instrument using 200 kV acceleration voltage. Fourier transform infrared (FTIR) spectra were measured with a Nicolet iS5 spectrometer (Thermo Fisher Scientific, USA) over the range of 4000–500 cm^{-1}. Thermomechanical analysis (TMA) for each film was carried out using a Discovery TMA 450 Thermomechanical Analyzer (TA Instruments, USA), with heating and cooling rates of 5 and 2 C min^{-1}, respectively. Breakdown tests were done using a PK-CPE1801 Ferroelectric Polarization Loop and Dielectric Breakdown Test System (PolyK, USA) equipped with a Trek High

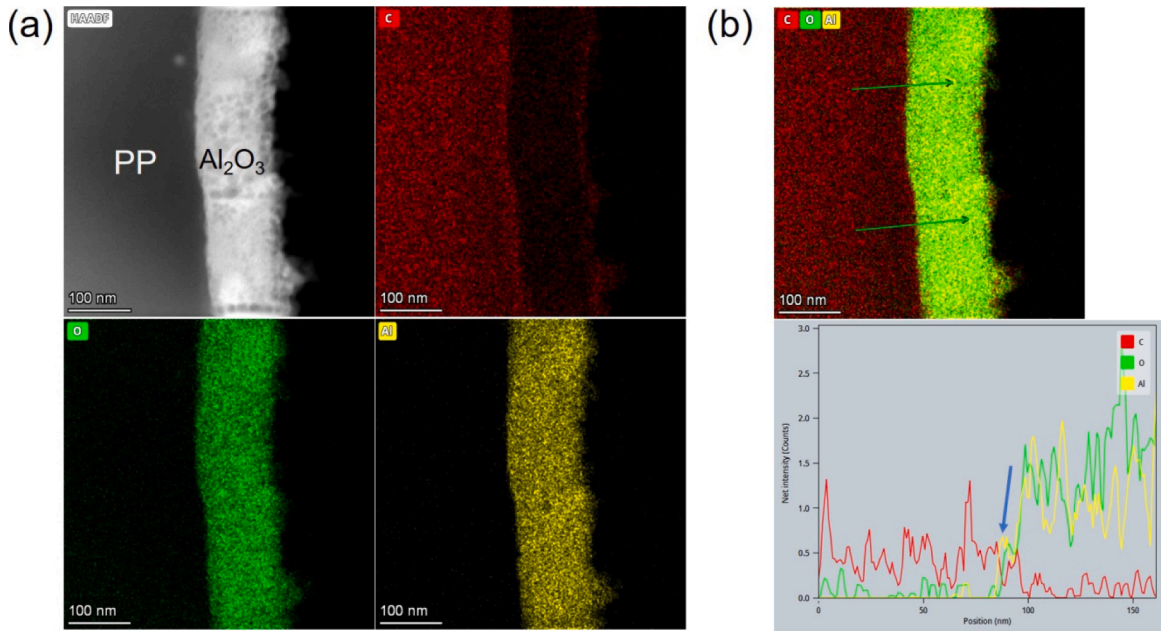

Fig. 2. (a) TEM images and element mapping of Al_2O_3 coated PP. (b) Distribution of elements on a straight line.

Voltage Amplifier (Model: 610E), along with a homemade sample holder soaked inside a constant-temperature oil bath system. Metal ball-plane electrode structure was used for breakdown measurement with the voltage rise rate of 500 V/s. Dielectric properties of the films were tested using a broadband dielectric impedance analyzer Concept 41 (Novocontrol, Germany) in the frequency range of 10 Hz–10^5 Hz. All films were dried for 3 h at 70 ℃ in a vacuum oven before the dielectric test.

2.4. Finite element simulation

COMSOL Multiphysics 5.6 was used to simulate the energy storage of flat PP capacitors. The thickness of PP and Al_2O_3 was set at 2.4 μm and 80 nm, respectively. For electric field simulation, the thickness of PP is set to about 1 μm and 20 nm Al_2O_3 layer.

3. Results and discussions

3.1. ALD coating effect on PP films

Atomic layer deposition is a method in which inorganic compounds can be deposited on a substrate in the form of a single atomic layer. The working diagram of ALD is shown in Fig. 1a. There are two storage jars containing precursor H_2O and TMA respectively. The valves will be opened alternately, and then precursors are sent to the vacuum chamber by argon. The chamber is filled with precursor molecules and adsorbed at any part of the film. As shown in Fig. 1b, argon will carry the aluminum precursor to the film surface, and then part of the non-adsorbed precursor will be taken away. Then water molecules enter the chamber and are adsorbed on the aluminum precursor. At this time, the two precursors will react to produce alumina and methane. The argon takes away the generated waste gas. At this point, a cycle reaction is completed, and then the same steps will continue. With the increase of the number of cycles, the thickness of the deposition will also increase.

$$2Al(CH_3)_3+3H_2O^{®}Al_2O_3+6CH_4 \quad (1)$$

Fig. 1c shows the SEM images of the PP film cross-section with an alumina coating layer. After 800 cycles of deposition, the alumina thickness is about 80 nm, which corresponds to 0.1 nm per cycle on average. The inset in Fig. 1c shows that both aluminum and oxygen elements were detected, proving that the deposition was alumina. A high-resolution, non-destructive AFM technique is used to inspect the subtle change of the surface roughness of the film [20,21], as shown in Fig. 2d. For baseline PP film, the arithmetical mean deviation of the roughness (Ra) is 10.7 nm, and the root means the square value of the roughness (Rq) is 14.8 nm while the coated film has the roughness of 18.4 nm and 23.4 nm, respectively. Such a small roughness variation before and after the ALD modification indicates the slight undulation of the film surface that is suitable for the subsequent metallization. The nucleation of Al_2O_3 ALD did not require the existence of additional specific chemical functional groups despite the possible assistance of minor OH on the polymers [22]. FTIR also shows the obvious peak of bulk Al_2O_3, and no other functional group peaks appeared indicating no additional chemical bonds (Fig.S2, Supporting Information).

ALD on polymers is known to involve infiltration of the precursors into the sub-surface of the film in general, in addition to coating outside the surface. To get a closer picture, the interface between PP film and coating layer is characterized by a cross-sectional elemental mapping, as shown in Fig. 2a. The high-angle annular dark-field (HAADF) image shows that the PP surface has a tight and sharp connection with the Al_2O_3 layer because no chink appears at the interface. O and Al elements are both detected in the same region indicating the uniformity of the ALD coating. Fig. 2b presents the elemental distribution across the interface. C element content decreases when O and Al content increases simultaneously while crossing the interface. It is noted that Al and O increase when C does not fall to zero in the Al_2O_3 layer, implying that the C penetration into Al_2O_3. TEM images also show that the inorganic deposition inside the tortuous surface of PP film resulting in a conformal contact. Such a steric configuration between polymer and Al_2O_3 coating may provide the role of limiting the PP chain movement particularly at high temperatures (to be discussed later). In addition, the deposited Al_2O_3 was found to be amorphous in nature using the ALD parameter in this work, as shown in Fig.S1, Supporting Information.

The dielectric breakdown strength, dielectric loss, and dimensional change of the dielectric polymer films are the key indicators of whether the films can be used by design engineers and the capacitor industry or not [23]. Dielectric breakdown is a statistic phenomenon, often described by the Weibull statistical model, $P(E) = 1 - \exp(-(E/a)^b)$, where P(E) is the probability of the films to breakdown at electric field E, a is the Weibull breakdown field at which 63.2% of the breakdown of the

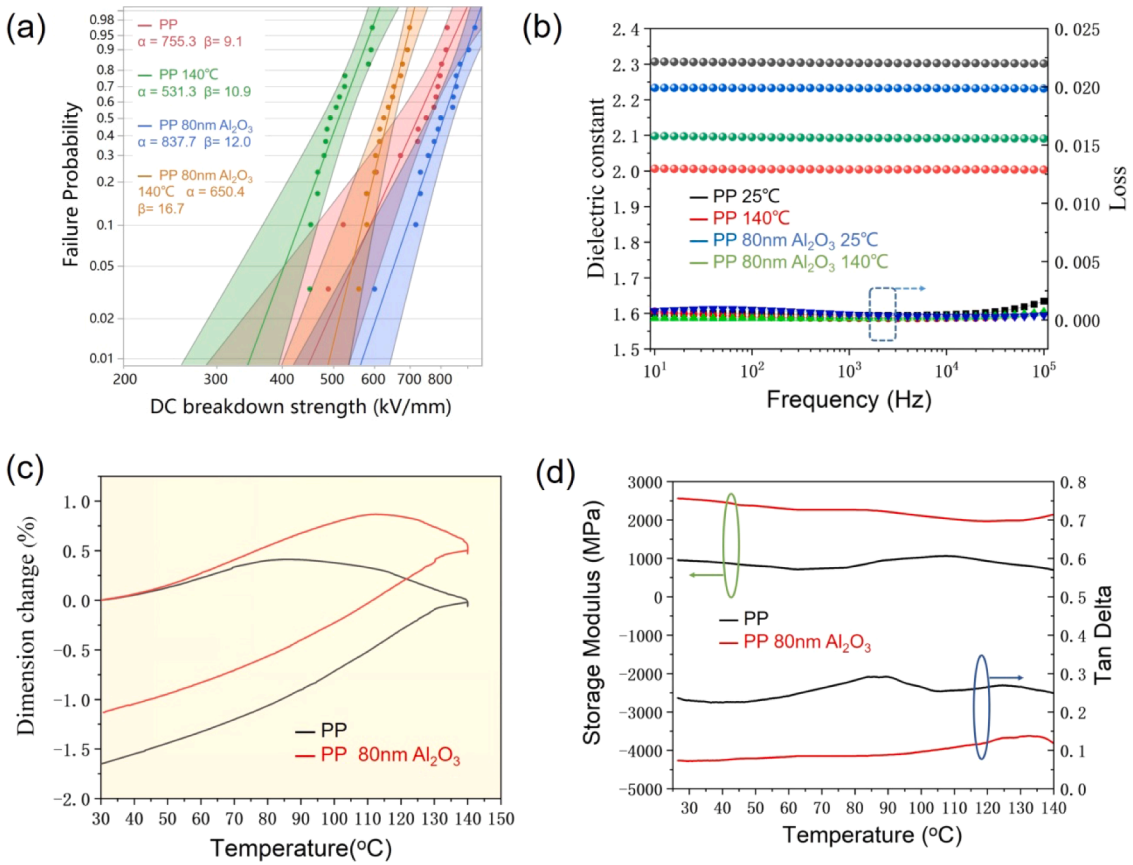

Fig. 3. (a) The Weibull distribution curves of PP and 80 nm Al_2O_3 coated PP at room temperature and 140 ℃. (b) Dielectric constant and loss of PP matrix and coated film samples. (c) Deformation of films from 30 ℃ to 140 ℃and isothermal for 1 h at 140 ℃. (d) Storage modulus and tan delta of PP and 80 nm Al_2O_3 coated PP.

film and b is the statistical spread of the breakdown field, also the slope of Weibull distribution curve [24,25]. Fig. 3a shows the positive effect of the ultra-thin oxide layer on the dielectric strength of the micron-thick PP films at room temperature and 140 ℃. Remarkably, the dielectric strength at 140 ℃ is increased by 22.4%. This increase was explained to be related to the higher dielectric constant of the coating layer that weakens the localized electric field in prior investigation [17]. Additionally, the breakdown strength of PP films with different coating thicknesses is shown in Fig.S3. Thicker coating leads to higher breakdown resistance but is not significant. Fig. 3b presents the difference between the dielectric constant and loss tangent of films. In the range of 25 ℃–140 ℃, the dielectric constant of PP films changes little with temperature, which indicates the good thermal stability of PP and coated PP films. As the temperature increases, the dielectric constant of PP decreases from 2.3 at 25 ℃ to 2.0 at 140 ℃. The dielectric constant of coated PP is slightly lower than that of PP at room temperature but slightly higher than that of PP at high temperature. PP's dielectric constant is lower than that of alumina and decreases with increasing temperature. Maintaining the higher dielectric constant at higher temperatures due to the coated alumina contribution is conducive to the energy storage of PP at high temperatures because energy density is $1/2\varepsilon_0\varepsilon_r E^2$, where E is the applied electric field, ε_r is the dielectric

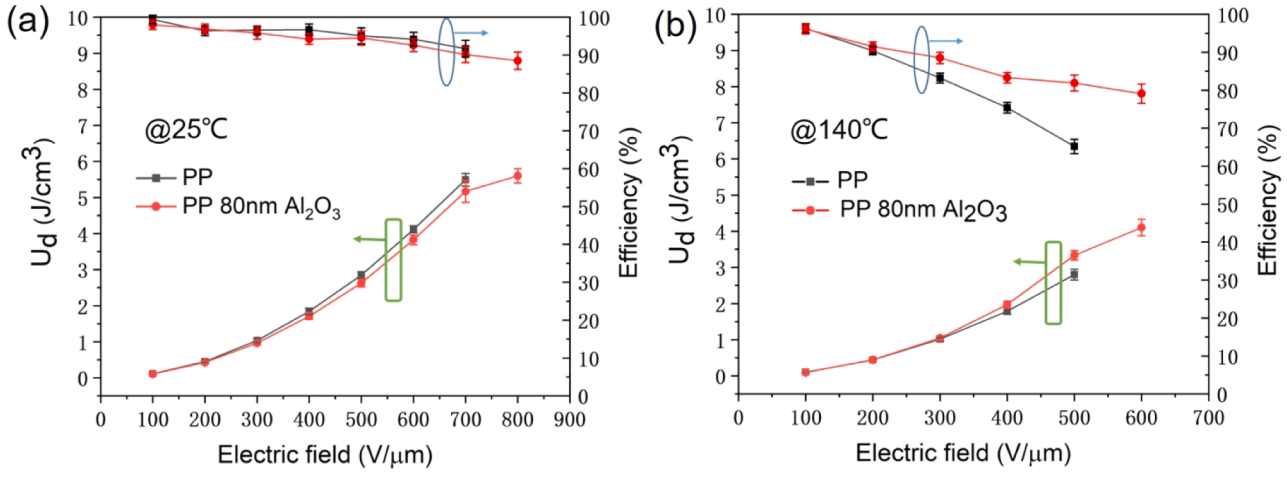

Fig. 4. (a,b) Discharged energy storage and efficiency of films at 25 ℃ and 140 ℃.

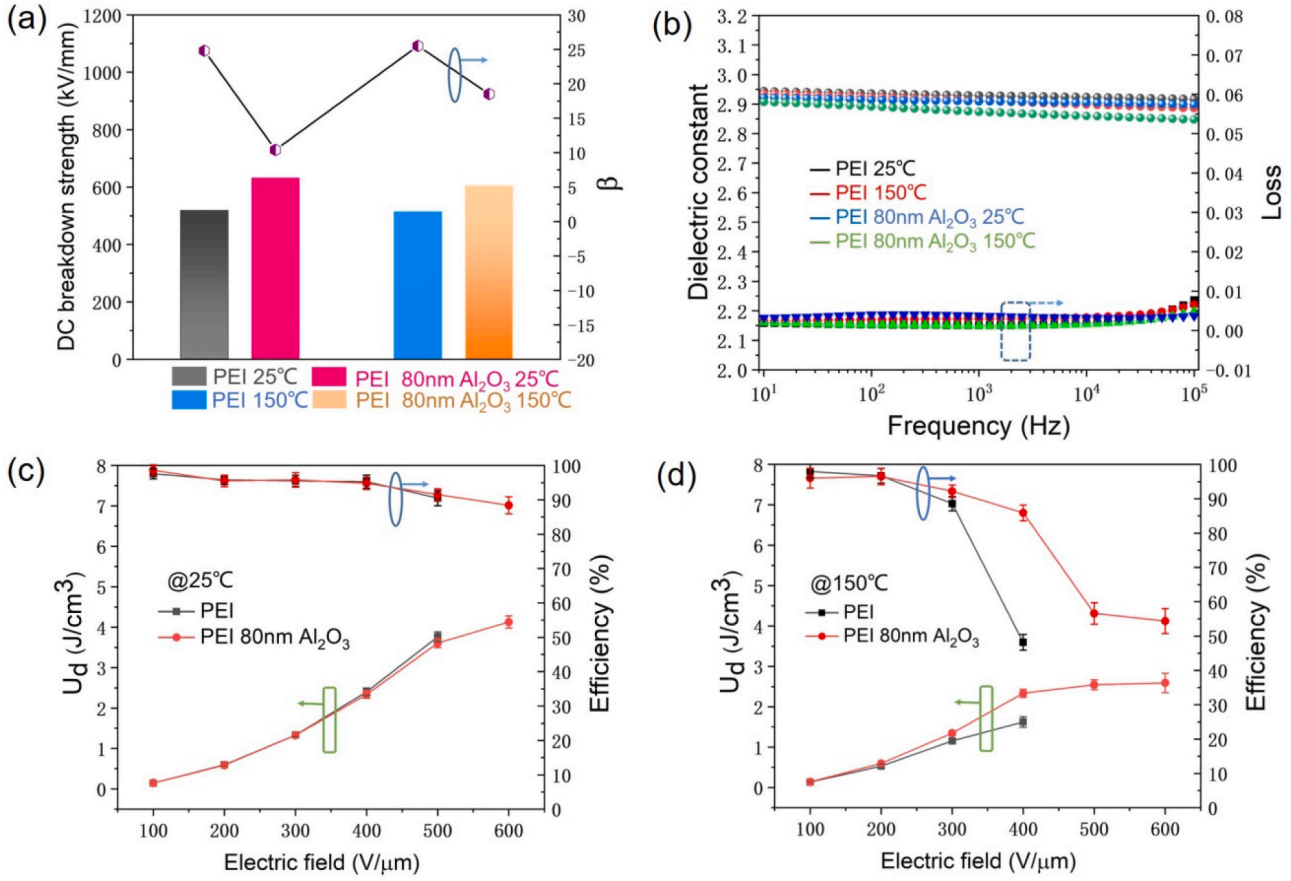

Fig. 5. (a) The breakdown strength of PEI film and 80 nm Al_2O_3 coated PEI film at room temperature and 150 ℃. (b) Dielectric constant and loss of PEI film and coated film samples. (c,d) Discharged energy storage and efficiency of films at 25 ℃and 150 ℃.

constant, and ε_0 is the vacuum permittivity (8.85×10^{-12} F/m). Interestingly, all films show ultralow dielectric loss below 0.001 with the frequency from 10 to 10^4 Hz. Fig. 3c illustrates the deformation in the machine direction of 5.8 μm PP films when testing up to 140 ℃, after one temperature cycle, the coat PP film only exhibits 1.1% size change while uncoated PP film shows 1.6%. The high deformation occurring at higher temperatures is one of the major reasons for the PP film not being suitable for high-temperature capacitor application despite the measurable breakdown strength at higher temperatures. Alumina coating makes it possible to serve the capacitor purpose because the alumina coating on the film surface limits the movement of molecular chain segments below the film surface. As a result, the PP films exhibit an increased storage modulus and reduced loss tangent, as shown in Fig. 3d. The storage modulus characterizes the elastic behavior of the material after deformation. The ratio of loss modulus to storage modulus is defined as the loss tangent, which reflects the anelastic or viscoelastic behavior of the material containing defects or molecular disorders. The enhanced storage modulus and steric hindrance between polymer and alumina coating explain why coated PP films can resist the deformation at higher temperatures [17].

In addition, the alumina-coated PP film possesses an outstanding energy storage capability at higher temperatures. Fig. 4a shows that the ultra-thin alumina coating does not inhibit the discharge performance of the film at room temperature, and the maximum discharge energy density (U_d) reaches 5.6 J/cm^3, slightly higher than 5.1 J/cm^3 of uncoated PP baseline. The advantage of alumina coating is more evident for the films tested at high temperatures. Fig. 4b shows that the coated film can still withstand the electric field strength of 600 V/μm at 140 ℃. In this higher temperature neighborhood, the discharged energy density (U_d) and efficiency (η) defined as the ratio of discharged energy to total charging energy of the coated films are much higher than those of uncoated PP at higher temperatures. For example, the U_d of the coated PP is 3.3 J/cm^3 and 4.1 J/cm^3 at 500 V/μm and 600 V/μm, while that of PP film 2.8 J/cm^3 at 500 V/μm, respectively, at 140 ℃. The corresponding efficiency is 81.9, 79.1, and 65.2, indicating less loss of the coated PP films than uncoated PP films. Therefore, the surface coating strategy provides an effective solution for the PP film to be stable for high-temperature capacitor applications.

3.2. ALD coating effect on PEI films

The ALD coating strategy of enhancing breakdown strength and modulus can be applied to many other polymer films, for instance, amorphous polyetherimide (PEI), a strong candidate dielectric material for its high-temperature stability and superior dielectric properties [26–28]. The nucleation of Al_2O_3 on PEI film is like that of PP except for a higher electrostatic nature due to polar groups for PEI that may enhance the initial nucleation (Fig.S2, Supporting Information). Applying the similar ALD coating scheme, the breakdown strength of PEI film coated with nanometer alumina rises by 21.8% at room temperature and 17.6% at 150 ℃, respectively, higher than those of uncoated PEI film, as shown in Fig. 5a. At 150 ℃, the breakdown strength of the coated film is more than 600 V/μm, which is outstanding among many polymer films. Fig. 5b shows the dielectric properties of PEI baseline and coated PEI at different temperatures. The dielectric constant of ALD coated PEI film is slightly lower than that of pure PEI. The small change of dielectric constant in the wide frequency range shows that the polarization can keep up with the change of frequency promptly. This frequency independence is an essential attribute of high-temperature capacitors. Interestingly, the loss of the coated PEI

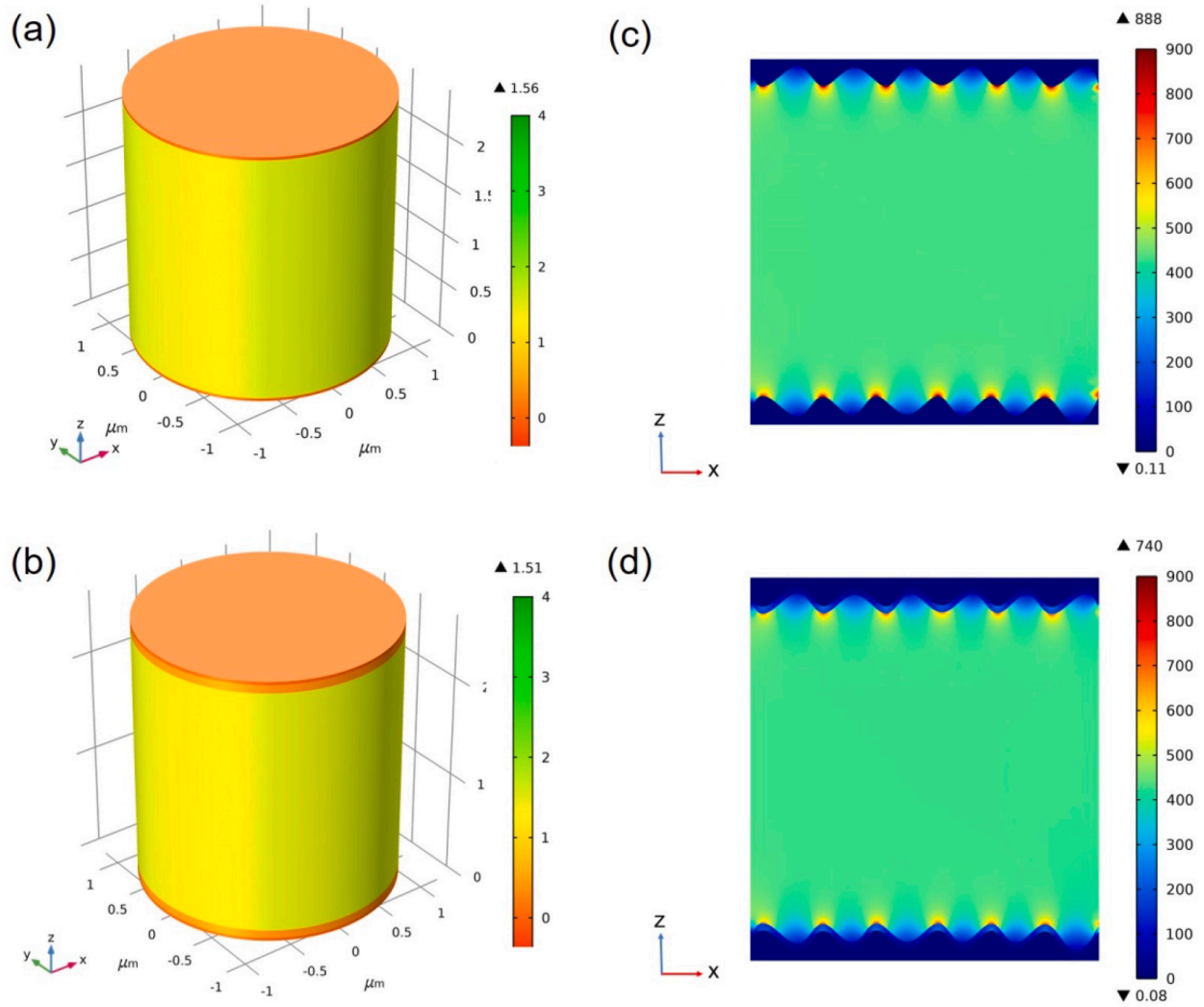

Fig. 6. Finite element simulation for (a-b) energy density with same voltage of 2.4 μm PP film and 80 nm Al_2O_3 coated PP film and (c,d) electric field distribution simulation of PP film with a rough surface and Al_2O_3 coated PP film.

film remains less than 0.005 even at 150 ℃ and 10^5 Hz, which is also favorable for high-performance capacitors. Fig. 5c shows that the ultra-thin alumina coating does not inhibit the discharge performance of the PEI film and the room temperature U_d reaches 4.13 J/cm^3, which is higher than 3.76 J/cm^3 of the uncoated PEI baseline according to polarization curves. As shown in Fig. 5d, the U_d and η of the coated film at 150 ℃ are higher than that of the PEI baseline as well. For example, the U_d of coated PEI is 2.33 J/cm^3 at 400 V/μm with an efficiency of 85.9% while that of PEI film is only 1.62 J/cm^3 with low efficiency of 48.2%, respectively. Furthermore, the coated film can withstand the electric field of 600 V/μm and maintain an ultralow deformation (<0.5%) (Fig. S4, Supporting Information), which is desirable for electrical insulation and capacitor applications. These results again present a clear message about the commonality of ALD coating on enhancing the dielectric strength and thermal stability of dielectric polymer films.

3.3. Computation study on breakdown mechanism

It has not been easy in understanding the dielectric breakdown mechanism of dielectric polymer films. The enhanced dielectric strength by surface oxide coating was associated with the higher dielectric constant of the coating layer that weakens the localized electric field in the past investigation. In addition, the observation of the increased elastic modulus leads to further understanding of the mechanism from the viewpoint of electrical-mechanical interaction. At higher temperatures, the thickness change induced by electric voltages can become more evident and is closely related to Young's modulus and applied voltage of the dielectric film. The dependence of the breakdown voltage on Young's modulus can be expressed in the following relations [29].

$$\varepsilon_0\left(\frac{V}{d}\right)^2 = Y\,Ln\left(\frac{d_0}{d}\right) \tag{2}$$

$$E_{BD} = \frac{d}{d_0}E_C \approx 0.6\sqrt{\frac{Y}{\varepsilon_0\varepsilon_r}} \tag{3}$$

Where V is the applied voltage, d_0 is the initial thickness, d is the decreased thickness after voltage application and Y is Young's modulus, Ec is critical electric stress. From Eqs. (2) and (3), smaller thickness change and higher Young's modulus are beneficial for enhanced breakdown strength. Therefore, ALD alumina coating caused the increase in storage modulus, reduced dimensional change, and then the increase in breakdown strength of dielectric films.

The finite element simulation is utilized to show the electrical and mechanical changes of materials before and after ALD coating based on the above analysis. The simulation assumes that both sides of PP and coated PP is sputtered with gold electrodes. As shown in Fig. 6a and b, the same voltage of 960 V is applied across the dielectric film (single

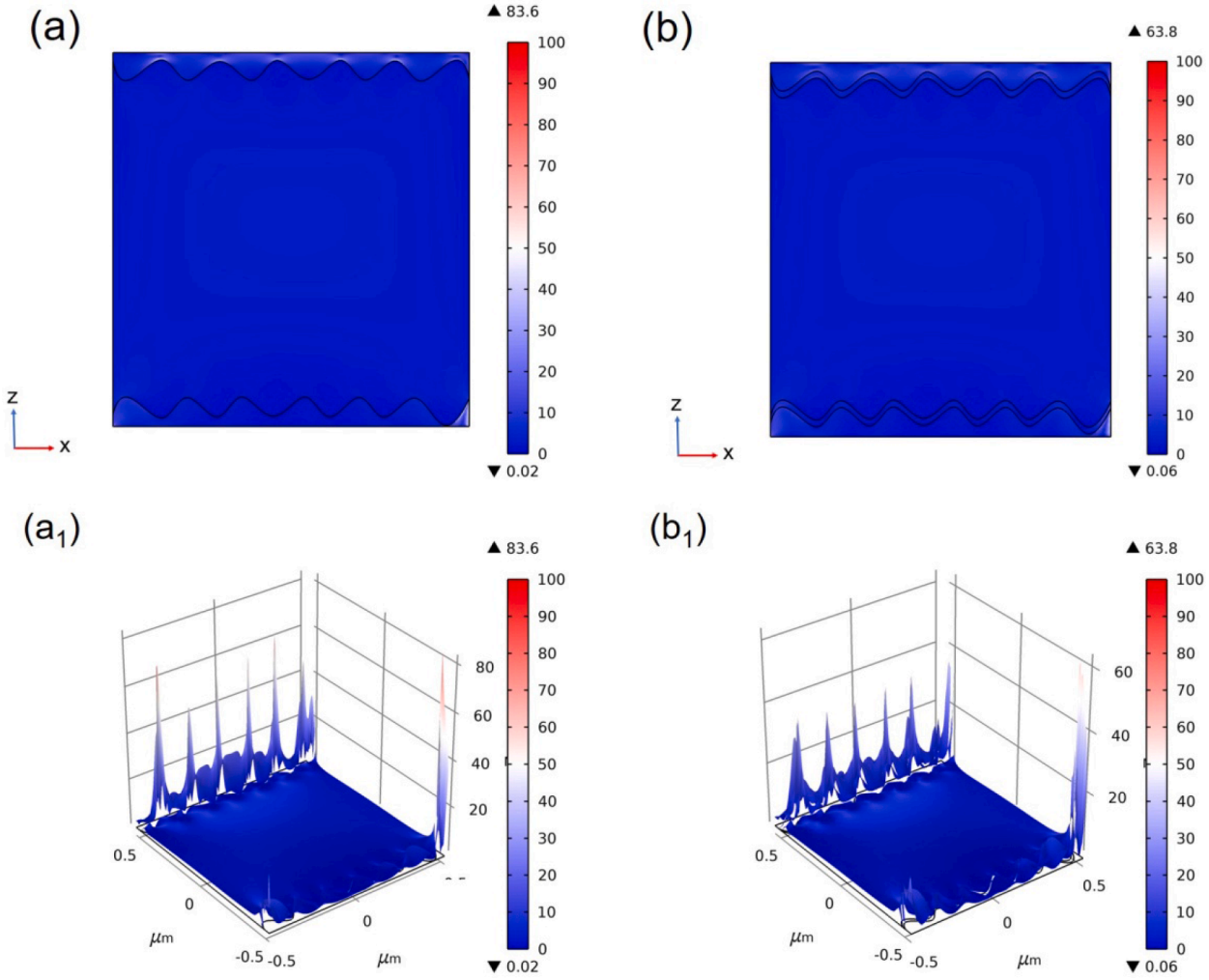

Fig. 7. Finite element method for (a–a_1) stress distribution of 1 μm PP film with a rough surface and (b–b_1) stress distribution of 20 nm Al_2O_3 coated PP film, value unit: MPa.

layer capacitor), and their energy storage densities are 1.56 and 1.51 J / cm^3, respectively (in the z-axis). The small change is consistent with the experimental results, where the PP films and the coated films show the subtle electrical difference at room temperature. In addition, the PEI and Al_2O_3 coated PEI films only exhibit the same nuances. (Fig.S5, Supporting Information) In order to truly reflect the rough surface of the actual PP film, the simulation of electric field distribution was conducted assuming the existence of gullies or pits on both sides of the film, as shown in Fig. 6c and d. The maximum electric fields of the PP and the coated PP appear at the tip of pits, which are 888 and 740 V/μm, respectively. Evidently, the alumina coating weakens the applied electric field and increases the breakdown strength.

Under an electric field, the film is subject to an electrical field-induced stress and then an inevitable deformation whose magnitude depends on the mechanical strength of the film. The electrical filed induced stress can be expressed by the following equation.

$$\sigma = 0.5\varepsilon_0\varepsilon_r E^2 \quad (4)$$

Where σ is mechanical stress. Eq. (3) implies that the total energy density is made up of electrostatic and electromechanical components [30]. Fig. 7 shows the results of the solid mechanic simulation of the coating effect on the dielectric films. The stress calculated from Eq. (2) at 600 V/μm is applied to the Y-axis of film and the stress distributions are presented in Fig. 7a and b. In order to display the simulation results more intuitively, the authors use the height to stand for the size of the value. The greater the height is, the greater the value is, as shown in Fig. 7a_1 and b_1. At constant electrical stress, the maximum von Mises stress (equivalent stress based on shear strain energy) of the PP film is 83.6 MPa at the edge, and that of the coated PP film is 63.8 MPa. This difference shows that the ALD alumina nanolayer can buffer the electrical stress and reduce the mechanical damage to the film. The ALD coating-induced stress effect is similar to that of the polytetrafluoroethylene (PTFE) film surface being flattened with epoxy resin that was disclosed in the previous work [31].

4. Conclusion

This work leverages the atomic layer deposition technique to deposit alumina on the surface of polypropylene and polyetherimide films to achieve improved dielectric and thermal-mechanical properties at higher temperatures. The alumina nanocoating effectively increased the breakdown strength and discharged energy density of the dielectric films in a wide temperature range. The discharge energy densities of polypropylene and polyetherimide reached 4.1 J/cm^3 and 2.6 J/cm^3 at 140 ℃ and 150 ℃, respectively. This strategy shows commonality in low-temperature crystalline PP and high-temperature amorphous PEI and thus may apply to other polymeric dielectric films. The dielectric strength enhancement was found to be also associated with the increased Young's modulus of dielectric films induced by the alumina coating. The finite element simulation supports the new perspective. The

ALD coating provides a promising way for dielectric polymer films and particularly low-temperature commercial films to withstand higher operating voltage and temperatures.

Declaration of Competing Interest

The authors declare that they have no known competing financial interests or personal relationships that could have influenced the work reported in this paper.

Acknowledgments

This work was supported by the Guangdong Department of Science and Technology Specialized Fund "Grant Project + Task List"-210728145861249 and Guangdong Province Science and Technology Department Major Project (Basic and Applied Research of Future functional materials under extreme conditions - 212019071820400001). The authors acknowledge the support of Zhixiang Si on TEM imaging.

Supplementary materials

Supplementary material associated with this article can be found, in the online version, at doi:10.1016/j.surfin.2021.101686.

References

[1] X. Wu, X. Chen, Q. Zhang, D.Q. Tan, Advanced dielectric polymers for energy storage, Energy Storage Mater. 44 (2022) 29–47.
[2] D.Q. Tan, Review of polymer-based nanodielectric exploration and film scale-up for advanced capacitors, Adv. Funct. Mater. 30 (2020), 1808567.
[3] M. Singh, I.E. Apata, S. Samant, W. Wu, B.V. Tawade, N. Pradhan, D. Raghavan, A. Karim, Nanoscale strategies to enhance the energy storage capacity of polymeric dielectric capacitors: review of recent advances, Polym. Rev. (2021) 1–50.
[4] W. Sun, J. Mao, S. Wang, L. Zhang, Y. Cheng, Review of recent advances of polymer based dielectrics for high-energy storage in electronic power devices from the perspective of target applications, Front. Chem. Sci. Eng. 15 (2021) 18–34.
[5] R.W. Johnson, J.L. Evans, P. Jacobsen, J.R. Thompson, M. Christopher, The changing automotive environment: high-temperature electronics, IEEE Trans. Electron. Packag. Manuf. 27 (2004) 164–176.
[6] J. Watson, G. Castro, A review of high-temperature electronics technology and applications, J. Mater. Sci. Mater. Electron. 26 (2015) 9226–9235.
[7] K. Bennion, M. Thornton, Integrated vehicle thermal management for advanced vehicle propulsion technologies, (2010).
[8] T.A. Burress, C. Coomer, S. Campbell, A. Wereszczak, J. Cunningham, L. Marlino, L. Seiber, H.T. Lin, Evaluation of the 2008 Lexus LS 600H Hybrid Synergy Drive System, Oak Ridge National Laboratory (ORNL), Oak Ridge, TN, 2009.
[9] J. Hsu, M. Staunton, M. Starke, Barriers to the Application of High-Temperature Coolants in Hybrid Electric Vehicles, Oak Ridge National Laboratory (ORNL, Oak Ridge, TN, 2006.
[10] H. Li, Y. Zhou, Y. Liu, L. Li, Y. Liu, Q. Wang, Dielectric polymers for high-temperature capacitive energy storage, Chem. Soc. Rev. (2021).
[11] Y. Zhou, Q. Wang, Advanced polymer dielectrics for high temperature capacitive energy storage, J. Appl. Phys. 127 (2020), 240902.
[12] Q. Zhang, X. Chen, B. Zhang, T. Zhang, W. Lu, Z. Chen, Z. Liu, S.H. Kim, B. Donovan, R.J. Warzoha, High-temperature polymers with record-high breakdown strength enabled by rationally designed chain-packing behavior in blends, Matter (2021).
[13] A. Oromiehie, H. Ebadi-Dehaghani, S. Mirbagheri, Chemical modification of polypropylene by maleic anhydride: melt grafting, characterization and mechanism, Int. J. Chem. Eng. Appl. 5 (2014) 117.
[14] A. Saha, V. Chakraborty, S. Chintalapudi, Chemical modification of polypropylene induced by high energy carbon ions, Nucl. Instrum. Methods Phys. Res. Sect. B 168 (2000) 245–251.
[15] M. Saule, L. Moine, M. Degueil-Castaing, B. Maillard, Chemical modification of polypropylene by decomposition of unsaturated peroxides, Macromolecules 38 (2005) 77–85.
[16] Y. Zhou, C. Yuan, S. Wang, Y. Zhu, S. Cheng, X. Yang, Y. Yang, J. Hu, J. He, Q. Li, Interface-modulated nanocomposites based on polypropylene for high-temperature energy storage, Energy Storage Mater. 28 (2020) 255–263.
[17] X. Wu, S. Tang, G. Song, Z. Zhang, D.Q. Tan, High-temperature resistant polypropylene films enhanced by atomic layer deposition, Nano Express 2 (2021), 010025.
[18] G. Song, D.Q. Tan, Atomic layer deposition for polypropylene film engineering—a review, Macromol. Mater. Eng. 305 (2020), 2000127.
[19] A. Azizi, M.R. Gadinski, Q. Li, M.A. AlSaud, J. Wang, Y. Wang, B. Wang, F. Liu, L. Q. Chen, N. Alem, High-performance polymers sandwiched with chemical vapor deposited hexagonal boron nitrides as scalable high-temperature dielectric materials, Adv. Mater. 29 (2017), 1701864.
[20] R. Garcia, Nanomechanical mapping of soft materials with the atomic force microscope: methods, theory and applications, Chem. Soc. Rev. 49 (2020) 5850–5884.
[21] G. Song, Y. Wang, D.Q. Tan, A review of surface roughness impact on dielectric film properties, IET Nanodielectr. (2021) 1–23.
[22] J. Ferguson, A. Weimer, S. George, Atomic layer deposition of Al_2O_3 films on polyethylene particles, Chem. Mater. 16 (2004) 5602–5609.
[23] D.Q. Tan, The search for enhanced dielectric strength of polymer-based dielectrics: a focused review on polymer nanocomposites, J. Appl. Polym. Sci. 137 (2020) 49379.
[24] W. Weibull, A statistical distribution function of wide applicability, J. Appl. Mech. 18 (1951) 293–297.
[25] L. Dissado, J. Fothergill, S. Wolfe, R. Hill, Weibull statistics in dielectric breakdown; theoretical basis, applications and implications, IEEE Trans. Electr. Insul. (1984) 227–233.
[26] X. Wu, D. Gandla, L. Lei, C. Chen, D.Q. Tan, Superior discharged energy density in polyetherimide composites enabled by ultra-low ZnO@ BN core-shell fillers, Mater. Lett. (2021), 129434.
[27] L. Ren, L. Yang, S. Zhang, H. Li, Y. Zhou, D. Ai, Z. Xie, X. Zhao, Z. Peng, R. Liao, Largely enhanced dielectric properties of polymer composites with HfO_2 nanoparticles for high-temperature film capacitors, Compos. Sci. Technol. 201 (2021), 108528.
[28] Q. Chi, Y. Zhou, Y. Feng, Y. Cui, Y. Zhang, T. Zhang, Q. Chen, Excellent energy storage performance of polyetherimide filled by oriented nanofibers with optimized diameters, Mater. Today Energy 18 (2020), 100516.
[29] K. Stark, G. Garton, Electrical strength of irradiation polymers, Nature 176 (1955) 1225–1226.
[30] J. Fothergill, Filamentary electromechanical breakdown, IEEE Trans. Electr. Insul. 26 (1991) 1124–1129.
[31] S. Luo, T.Q. Ansari, J. Yu, S. Yu, P. Xu, L. Cao, H. Huang, R. Sun, Enhancement of dielectric breakdown strength and energy storage of all-polymer films by surface flattening, Chem. Eng. J. 412 (2021), 128476.